A New Paradigm for Non-Geostationary Satellite Communications and Radio Astronomy System

Hlaing Minn, Dong Han and Yucheng Dai
Department of Electrical and Computer Engineering, University of Texas at Dallas, USA
Email: hlaing.minn@utdallas.edu, dong.han6@utdallas.edu, yucheng.dai@utdallas.edu

***Abstract*—This paper proposes a new paradigm to accommodate the rapid growth of non-geostationary orbit (NGSO) satellite communications system (SCS) and radio astronomy system (RAS). Traditionally, SCS and RAS are operated in different frequency bands to avoid radio frequency interference (RFI). However, the prospects of large-scale NGSO satellites cast a distressful RFI scenario to the ground-based RAS observations. By integrating SCS and RAS into the NGSO satellite system, the proposed paradigm mitigates the RFI significantly, enables plenty of new observation opportunities and capabilities for RAS, provides higher throughput for SCS, and creates potential new services/revenues for SCS. Potential deployment scenarios are discussed. In addition, the paper addresses two related problems of the new paradigm, namely the spectrum resource allocation problem and the RAS data transport problem. Simulation results demonstrate the performance advantages of the proposed paradigm and related solutions.**

I. Introduction

Non-geostationary orbit (NGSO) satellite communication systems (SCSs), namely Low Earth Orbit (LEO) and Medium Earth Orbit (MEO) systems, have been investigated for decades. However, the unsuccessful commercial applications of the former NGSO systems launched decades ago have reduced further effort to promote such systems for years [1]. Recently, due to the increasing demand for ubiquitous high-speed and low-latency internet connections as well as the rapid development of low-cost commercial spacecraft launching [2], [3], the space industry is energized with substantial efforts to launch thousands of NGSO satellites. For instance, companies such as OneWeb and SpaceX are proposing to launch thousands of LEO and MEO satellites [4], [5]. These future NGSO satellites will form a tremendous space backhaul network via inter-satellite links (ISLs) [6] as well as a ubiquitous wireless access network.

However, the prospects of such large-scale NGSO SCSs cast a distressing RFI situation to RAS. The ground-based RAS uses highly sensitive receivers to observe very weak signals from cosmic sources within a wide frequency range. Out-of-band spectrum sidelobes from satellite transmitters, which are negligible to other communication systems, could substantially disrupt radio astronomical observations (RAO). Furthermore, due to inherent nonlinearity of some transmitter components as well as device imperfection, unintended/unexpected RFI from satellites to RAS can occur. Although some efforts have been made to mitigate the RFI from active wireless services to the ground RAS [7]–[13], unfortunately, their applicability to the large-scale NGSO systems is very limited. As large-scale NGSO systems plan to cover most of the earth surface ubiquitously, radio observatories on earth cannot hide from NGSO satellites' potential RFI. As an example, we can recall the Iridium satellite system with 66 LEO satellites launched in 1998. Even though several attempts were made to avoid RFI to RAS, in practice RAO data were corrupted by Iridium's RFI as confirmed in the new measurements conducted in 2010 [14].

Higher resolution and sensitivity are the key performance metrics for RAS, where the former results from larger distances between different RAS antennas and the latter is achieved by increasing the overall antenna area to noise temperature ratio [15]. Besides, ground RAS cannot make observations in certain frequency bands due to the large atmospheric attenuation. In this regard, space-based radio telescopes are very attractive solutions. For instance, Japan launched a satellite for the Very Long Baseline Interferometry (VLBI) Space Observatory Program (VSOP) in a highly elliptical orbit with an apogee altitude of 21,400 km and a perigee altitude of 560 km in 1997 [16] and Russia launched a satellite named RadioAstron to an elliptical orbit with a perigee of 10,000 km and an apogee of 390,000 km in 2011 [17]. Both of them can form a VLBI with the ground radio telescopes to increase the RAO performance.

Motivated by both the critical conflict between the next generation NGSO SCS and RAS and the higher performance demands of RAS, we propose to develop a new paradigm which overcomes the issues of the existing paradigm and offers several additional advantages. The new paradigm changes NGSO SCS into an integrated NGSO satellite communication and radio astronomy system (SCRAS) where satellites provide both RAO and communication services. The direct benefits are that RAS gains more RAO opportunities and performance enhancements (in terms of sensitivity through combining as in [18] and [19] and resolution through VLBI) and SCS obtains higher throughput and new services or business opportunities. The proposed approach offers a new infrastructure and paradigm at the side of data acquisition from radio astronomical objects. It is in synergy with the recent development of virtual astronomy observatory (VAO) [20] which is at the data processing side, offering a large scale electronic integration of radio astronomy data and tools for radio astronomers.

This paper is organized as follows. Section II describes the new paradigm, its benefits to both SCS and RAS, potential deployment scenarios and challenges. We address the resource

978-1-5386-3180-5/18/$31.00 ©2018 IEEE

allocation problem in Section III and the RAO data transport problem in Section IV. Finally, Section V concludes this paper.

II. New Paradigm and Deployment Scenarios

In the proposed paradigm, the communication satellites will be equipped with additional antennas and receivers to make RAO in addition to their main communication services. The zone for active communication services is towards the earth from the satellites while the one for RAO is from the satellites outwards the earth. The satellites can use the RAO spectrum also in their active communication services as the spatial zones for the two services are non-interfering. Similarly, RAO can be made in the band for active wireless service. In other words, the communication satellites in the proposed paradigm now take the role of radio telescopes on earth for RAO in exchange for their spectrum uses of the RAO spectrum for active communication systems. Satellites need to make RAO at a mutually agreed data rate and forward their RAO data through their earth-station gateways to RAS. This innovation will benefit the NGSO SCS in the following aspects:

- The bands in which NGSO systems can make sufficient RAO can be reused for active wireless services, thus offering more spectrum access opportunities for SCS.
- For the above bands, SCS will no longer need to implement RFI-avoiding mechanisms.
- SCS systems can obtain new services/business opportunities for additional RAO beyond their obligation.

The proposed paradigm offers the following benefits to RAS:

- RAO from the satellites has signal strength gain due to the removal of atmospheric attenuation.
- The bands allocated for active wireless services which typically do not yield meaningful RAO at the ground telescopes can now be observed for RAS measurements.
- RFI from consumer electronic equipment and wireless systems, which are difficult to prevent from happening in practice, would not affect the RAO of the satellites.
- Due to large-scale NGSO systems, large-scale RAS telescope arrays infeasible with ground telescope systems can be realized.
- Large-scale NGSO satellites provide more RAO time than ground-based radio observatories.

Fig. 1 illustrates potential RFI to RAS in the two paradigms. In the existing paradigm, ground telescopes could be affected by RFI from terrestrial transmitters as well as all satellites. In the proposed paradigm, NGSO satellite based telescopes are not affected by terrestrial transmitters but potentially only by above-altitude satellite systems. Both LEO and MEO satellites are the candidates for our proposed paradigm. For the radio telescopes on a certain orbit, the RFI caused from the downlink transmissions of higher satellites in the same frequency cannot be neglected. For instance, Fig. 1 shows that the geostationary orbit (GSO) satellites' downlink transmissions potentially interfere all the radio telescopes on MEO, LEO and the ground. Similarly, the MEO satellites' downlink transmissions impact both the LEO and the ground radio telescopes. To avoid the

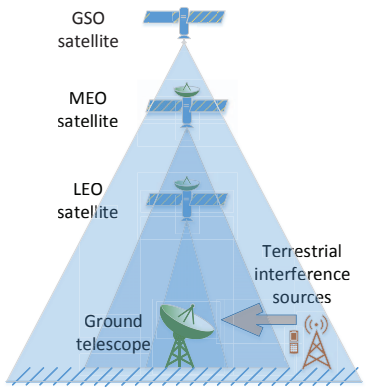

Fig. 1. Potential RFI to RAS in the existing paradigm (ground telescopes) and the proposed paradigm (LEO/MEO based telescopes)

RFI from the GSO satellites, the radio telescopes on NGSO satellites may use different frequency. In general, the MEO-RAS would be subject to less RFI than the LEO-RAS. But we note that there is high possibility for the LEO-RAS to avoid the RFI caused by MEO downlink transmissions, since the ocean covers over 70 percent of the earth surface where the satellite downlink transmissions are very rare. Considering the industry's main interest in LEO systems and availability of the LEO system information, we take the OneWeb's LEO system as an example in this paper but our paradigm and analysis also work for other NGSO-RASs.

The LEO constellation proposed by OneWeb have 18 separated orbit planes and 40 equally separated satellites on each orbit plane, where the satellites in a neighbor orbit are offset by 4.5 degrees to increase the overall coverage. All satellites have the same height of 1200 km and the same inclination angle of 87.9 degrees [21]. The ground gateways are assumed to be uniformly distributed on lands between latitudes of $70^{\circ}\mathrm{N}$ and $70^{\circ}\mathrm{S}$. We assume the minimum elevation angle, above which any associated gateway can transmit to a NGSO satellite, is 30 degrees for this system.

To provide attractive incentives to both SCS and RAS communities, the frequency bands for the proposed paradigm can include the bands allocated to NGSO SCS and those allocated to RAS or some new bands. In view of the recent Federal Communications Commission (FCC)'s approval of the frequency bands for OneWeb's NGSO SCS which are shown in the first column of TABLE I [22], [23], these bands are excellent candidates for the proposed paradigm. We note that the four links of this SCS, namely user to satellite (US), satellite to user (SU), earth-station gateway to satellite (GS), and satellite to gateway (SG), use frequency division duplexing (FDD) and frequency division multiplexing (FDM). Additional new or RAS band(s) can be either separate bands or a single band. As an example, the third column of TABLE I shows four bands which are currently allocated to RAS on the primary basis as four new bands added to the proposed NGSO SCRAS. We will also consider an alternative scenario with a single new band having the same total bandwidth as the four RAS bands. In terms of spectrum access, we will use FDD+FDM for

TABLE I. An Example of Frequency Allocation for the Proposed Paradigm

Original Bands (GHz)	Bandwidth B_n (GHz)	New FDD Bands (GHz)	Bandwidth ΔB_n (GHz)	Link (n)
10.7-12.7	2.0	10.6 - 10.7	0.1	User downlink (SU)
12.75-13.25 14.0-14.5	1.0	15.35 - 15.4	0.05	User uplink (US)
17.8-18.6 18.8-19.3 19.7-20.2	1.8	22.21-22.5 23.6-24	0.69	Gateway downlink (SG)
27.5-29.1 29.5-30.0	2.1	31.3-31.8	0.5	Gateway uplink (GS)

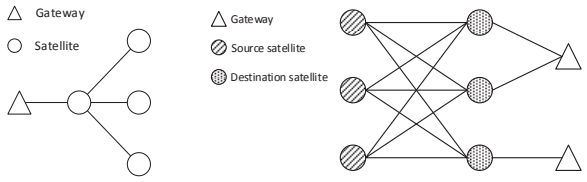

(a) (b)

Fig. 2. System topological graphs. (a) Local topological graph for resource allocation with $M = 4$. (b) Topological graph for RAO data transport with $L = 2$ and $N_s = N_d = 3$ (In practice, N_s could be greater than N_d).

separate bands and time division duplexing (TDD)+FDM/time division multiplexing (TDM) for the single band.

As combined spectrum from RAS and SCS is used for both services in the proposed paradigm, two technical challenges arise. The first one is how to allocate resources between the RAS and SCS services. The second challenge is how to efficiently transport RAO data to the earth-station gateways. Since SCS throughput, quality-of-service constraint and RAO data rate support are inter-related in the proposed paradigm, we will study them in more details in addressing the two challenges in the next sections. We note that there are several other challenges for the proposed paradigm including changes in regulatory domain, satellite designs, and cooperation between SCS and RAS communities, which are outside the scope of this paper. For convenience, a list of the key parameters in this paper are shown in TABLE II.

III. Spectrum Resource Allocation for SCRAS

A. Development of Resource Allocation

We will first develop a system model that captures the essence of the spectrum allocation and related achievable data rate. For this, instead of considering all satellites and all earth-station gateways altogether, we start with analyzing the throughput involving only one typical gateway antenna (i.e., one pair of SG and GS links). Suppose the SG (GS) link carries the traffics of M satellites, of which only one satellite is directly connected to the gateway antenna and the other $M-1$ satellites. In other words, the directly connected satellite serves as a relay for the traffics from (to) other satellites. The connections between satellites are via inter-satellite links (ISLs). An example of the topological graph is shown in Fig. 2(a) to illustrate the connectivities we consider in this section. We note that M can fluctuate across time, antenna dishes and gateways. But for our spectrum allocation and achievable data rate evaluation purpose, we can consider a fixed value of M.

We regard the traffics from multiple users within one satellite coverage as an aggregate traffic so that the SU broadcast link and the US multiple access link are simplified to point-to-point links. Besides, a fixed data rate R_{RAS}/M is reserved for RAO data downlink transmission for each satellite which results in an aggregate RAO data rate of R_{RAS} in the SG link. We denote the aggregate SCS traffics in terms of packets per second for the M satellites as independent and identical distributed (i.i.d.) Poisson random variables [24]–[27], $x_i,\ i = 1, \ldots, M$. The packet sizes are denoted as $\{\gamma_{\mathrm{n}},\ \mathrm{n} \in \mathcal{N}\}$, where $\mathcal{N} = \{\mathrm{SU}, \mathrm{US}, \mathrm{GS}, \mathrm{SG}\}$ indicates the four different links. Furthermore, the SCS data rate demands for the considered links are

$$r_{\mathrm{n},i} = \gamma_{\mathrm{n}} x_i, \quad \mathrm{n} \in \{\mathrm{SU}, \mathrm{US}\},\ i = 1, \ldots, M \tag{1}$$

$$r_{\mathrm{m}} = \gamma_{\mathrm{m}} \sum_{i=1}^{M} x_i, \quad \mathrm{m} \in \{\mathrm{SG}, \mathrm{GS}\}. \tag{2}$$

The satellites apply beam arrays and polarized antennas which result in different multiplexing gains, $\{G_{\mathrm{n}} :\ \mathrm{n} \in \mathcal{N}\}$. Similarly, the four links also have individual spectrum efficiencies $\{\eta_{\mathrm{n}}\}$ and frequency reuse factors $\{\beta_{\mathrm{n}}\}$. Given the original band $B_{\mathrm{n}},\ \mathrm{n} \in \mathcal{N}$ shown in the first column of TABLE I, the capacity of each link in the existing paradigm can be represented as

$$C_{\mathrm{n}} = \frac{\eta_{\mathrm{n}} G_{\mathrm{n}}}{\beta_{\mathrm{n}}} B_{\mathrm{n}}, \quad \mathrm{n} \in \mathcal{N}. \tag{3}$$

Now, consider the proposed paradigm with the original bands of SCS in the first column and additional new bands in the third column of TABLE I. This case can be denoted by "new FDD bands". Another deployment scenario is to use a single new band with the same total bandwidth instead of four new bands, and it will be called "new TDD band".

Suppose the total bandwidth of the new band(s) is ΔB and the fraction of this resource allocated to the link n is denoted by α_{n}. Then, for the new FDD bands, $\{\alpha_{\mathrm{n}}\}$ are fixed with $\sum_{\mathrm{n}\in\mathcal{N}} \alpha_{\mathrm{n}} = 1$ since the bandwidth $\Delta B_{\mathrm{n}} = \alpha_{\mathrm{n}} \Delta B$ of link n is fixed. However, for the new TDD band, the resource allocation is done in terms of frame partitioning (TDM) and hence, $\{\alpha_{\mathrm{n}}\}$ can be optimized. As with any TDD system, guard time intervals are needed in this case. We

TABLE II. List of Key Symbols

Symbol	Definition
$\mathcal{C}$	Center of RAO area
L	Number of gateways selected for RAO data downloading
N_d	Number of (destination) satellites connected to the selected gateways
N_s	Number of (source) satellites selected for RAO
$\beta_{\rm US},\ \beta_{\rm SU},\ \beta_{\rm GS},\ \beta_{\rm SG}$	Frequency reuse factor of US, SU, GS and SG links
$\eta_{\rm US},\ \eta_{\rm SU},\ \eta_{\rm GS},\ \eta_{\rm SG}$	Spectrum efficiency (bits/s/Hz) of US, SU, GS and SG links
$\gamma_{\rm US},\ \gamma_{\rm SU},\ \gamma_{\rm GS},\ \gamma_{\rm SG}$	Packet size (Mbits) of US, SU, GS and SG links
$\alpha_{\rm US},\ \alpha_{\rm SU},\ \alpha_{\rm GS},\ \alpha_{\rm SG}$	Resource allocation factor of US, SU, GS and SG links
$G_{\rm US},\ G_{\rm SU},\ G_{\rm GS},\ G_{\rm SG}$	Multiplexing gains of US, SU, GS and SG links

denote $T,\ T_{\rm guard}$ and $T_{\rm n},\ {\rm n}\in\mathcal{N}$ as the total number of subframes in one frame, the number of subframes allocated for guard intervals in one frame and the number of subframes allocated for link n in one frame. In other words, we have $T=\sum_{{\rm n}\in\mathcal{N}}T_{\rm n}+T_{\rm guard}$, $\alpha_{\rm guard}=\frac{T_{\rm guard}}{T}$ and $\alpha_{\rm n}=\frac{T_{\rm n}}{T},\ {\rm n}\in\mathcal{N}$. We can write equivalent bandwidths of the four links for the new TDD case as $\{\Delta B_n=\alpha_n\Delta B\}$ to unify parameters for the new FDD bands and the new TDD band. Note that $\alpha_{\rm guard}=0$ for the new FDD bands. Then, the capacity achieved by the link n in the proposed paradigm is given as

$$\tilde{C}_{\rm n}=\frac{\eta_{\rm n}G_{\rm n}}{\beta_{\rm n}}\left(B_{\rm n}+\alpha_{\rm n}\Delta B\right),\quad {\rm n}\in\mathcal{N}. \tag{4}$$

For convenience, we denote function $F(\lambda,K)\triangleq\sum_{k=0}^{K}\frac{\lambda^k}{k!}e^{-\lambda}$ as the CDF of a Poisson distribution of which the mean is λ. Correspondingly, two inverse CDFs of a Poisson distribution are denoted as

$$F_{\lambda}^{-1}(p,K_0)\triangleq\max\left\{\lambda:F(\lambda,K_0)\le p\right\} \tag{5}$$

$$F_{K}^{-1}(p,\lambda_0)\triangleq\max\left\{K:F(\lambda_0,K)\le p\right\} \tag{6}$$

where F_{λ}^{-1} returns the mean of a Poisson distribution given the CDF value p and the upper bound K_0 and F_{K}^{-1} returns the upper bound K given the CDF value p and the mean λ_0.

With the new capacity $\tilde{C}_{\rm n}$ and the data rate demands shown in (1)-(2), we define an outage event of a link as the data rate demand being more than the capacity, and the outage probability is thereby represented as

$$P_{{\rm out,n}}=\mathbb{P}\left(r_{{\rm n},i}>\tilde{C}_{\rm n}\right),\ {\rm n}\in\{{\rm SU,US}\},\ i=1,\ldots,M \tag{7}$$

$$P_{{\rm out,m}}=\mathbb{P}\left(r_{\rm m}>\tilde{C}_{\rm m}\right),\ {\rm m}\in\{{\rm SG,GS}\}. \tag{8}$$

We mention the outage probabilities $\{P_{\rm out,n}\}$ for all the M SU (US) links are the same since the traffic $x_i,\ i=1,\ldots,M$ are i.i.d. Poisson random variables, and hence, we will skip satellite index i in the rest. Therefore, to satisfy the same outage probability constraint ϵ on the four links, the maximum achievable average SCS data rates can be given as

$$R_{\rm n}=\gamma_{\rm n}F_{\lambda}^{-1}\left(1-\epsilon,\frac{\tilde{C}_{\rm n}}{\gamma_{\rm n}}\right),\quad {\rm n}\in\{{\rm SU,US,GS}\} \tag{9}$$

$$R_{\rm SG}=\gamma_{\rm SG}F_{\lambda}^{-1}\left(1-\epsilon,\frac{\tilde{C}_{\rm SG}-R_{\rm RAS}}{\gamma_{\rm SG}}\right) \tag{10}$$

where $R_{\rm RAS}$ is the reserved data rate for RAO data downlink transmission. Assuming the average traffic ratio between the user downlink and uplink is $\zeta=\frac{\gamma_{\rm SU}}{\gamma_{\rm US}}$, we have

$$R_{\rm SU}=\zeta R_{\rm US}\quad\text{and}\quad R_{\rm GS}=\zeta R_{\rm SG} \tag{11}$$

where the second equation comes from that all the user downlink (uplink) data comes from the GS (SG) link. Due to the cascaded nature of the links between users and gateways, the maximum achievable average throughputs for the cascaded gateway-satellite-user (GSU) link, $\mathbb{T}_{\rm GSU}$, and the cascaded user-satellite-gateway (USG) link, $\mathbb{T}_{\rm USG}$, can be given by

$$\mathbb{T}_{\rm GSU}=\min\left(R_{\rm GS},MR_{\rm SU}\right) \tag{12}$$

$$\mathbb{T}_{\rm USG}=\min\left(R_{\rm SG},MR_{\rm US}\right). \tag{13}$$

With equations (11), (12) and (13), a sum throughput maximization problem is formulated as

$$\max_{\{\alpha_{\rm n}:\ {\rm n}\in\mathcal{N}\}}\quad \mathbb{T}_{\rm GSU}+\mathbb{T}_{\rm USG} \tag{14a}$$

$$\text{s.t.}\quad R_{\rm SU}=\zeta R_{\rm US},\ R_{\rm GS}=\zeta R_{\rm SG} \tag{14b}$$

$$\sum_{{\rm n}\in\mathcal{N}}\alpha_{\rm n}+\alpha_{\rm guard}=1. \tag{14c}$$

Since the constraints in (14b) are not closed-form functions of the optimization variables, we exhaustively search all the possibilities of $\{\alpha_{\rm n},{\rm n}\in\mathcal{N}\}$ with desired resolution (e.g., $1/T$ for the new TDD band).

B. Resource Allocation Performance Results

In the simulation, we define the spectrum efficiencies as $\eta_{\rm US}=1$, $\eta_{\rm SU}=1$, $\eta_{\rm GS}=4$ and $\eta_{\rm SG}=2$ bits/s/Hz[1] and the frequency reuse factors as $\beta_{\rm US}=4$, $\beta_{\rm SU}=4$, $\beta_{\rm GS}=1$ and $\beta_{\rm SG}=1$ [21]. The packet sizes are set to be $\gamma_{\rm US}=5$, $\gamma_{\rm SU}=10$, $\gamma_{\rm GS}=10$ and $\gamma_{\rm SG}=5$. The average traffic ratio between the user downlink and uplink is $\zeta=2$. According to [21], the multiplexing gains (the number of beams) of the four links are $G_{\rm US}=16,\ G_{\rm SU}=16,\ G_{\rm GS}=2$ and $G_{\rm SG}=2$. These settings will not change when the new frequency resources are added. The allocated bands in FDD mode are listed in the third column of TABLE I with a total bandwidth of 1.34 GHz. A continuous band with the same bandwidth is considered for TDD mode. In addition, we assume the total frame length in TDD mode is 100 ms, each frame consists of 100 subframes and 11 subframes are reserved for the guard interval between different links, i.e., $T=100$ and $T_{\rm guard}=11$.

Fig. 3 shows the relationship between the achievable RAO data rate and the local SCS throughput for three scenarios: i) only using original frequency resources assigned for the SCS (existing paradigm if $R_{\rm RAS}=0$), ii) adding new frequency resources in a fixed FDD scheme (new paradigm with new FDD bands) and iii) adding new frequency resources in a TDD

[1]We use a conservative setting in our numerical evaluation. In practice, the spectrum efficiency depends on the several system settings such as the modulation type and the SNR.

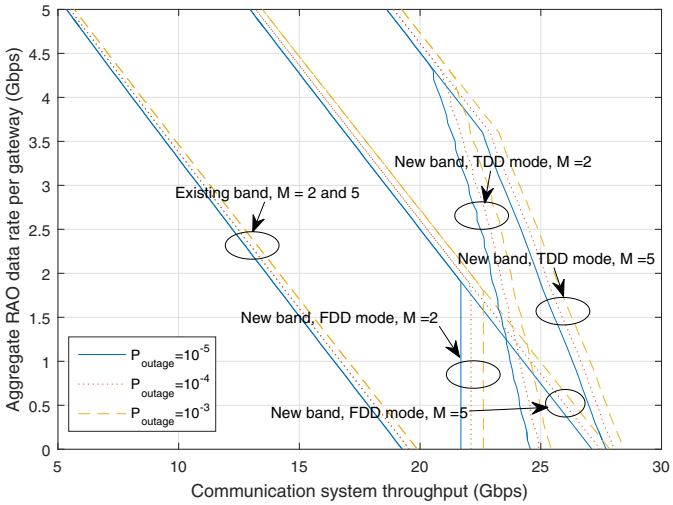

Fig. 3. Achievable RAO data rate and local SCS throughput

scheme with optimal frame partitioning (new paradigm with a new TDD band). To be specific, from Fig. 3 we can see that higher communication outage probability corresponds to a larger aggregate RAO data rate for the same SCS throughput. Besides, the optimized TDD resource allocation achieves the best performance as it always results in the highest RAO data rate given the same SCS throughput, outage probability and the number of satellites supported by the gateway.

The SCS throughput for the existing bands at the aggregate RAO data rate of zero corresponds to the scenario of the existing paradigm where the NGSO SCS does not perform RAS observation, e.g., the SCS throughput at $P_{\text{out}} = 10^{-3}$ is about 20 Gbps based on the total bandwidth of $B = 6.9$ GHz. When new bands with the total bandwidth of $\Delta B = 1.34$ GHz are added and if the aggregate RAO data rate of 2 Gbps per gateway antenna in the RAS observable zone is to be supported, then the achievable SCS throughput for the scenario with FDD new bands is about 22 Gbps and that for the scenario with the TDD new band is about 24 Gbps (26 Gbps) when $M = 2$ ($M = 5$), thus providing larger throughput to SCS than the existing paradigm.

Moreover, Fig. 3 also indicates how the bottleneck of the local system throughput is affected by the aggregate RAO data rate and the number of satellites supported by the gateway. On one hand, the increase of RAO data rate will reduce the SCS throughput. For instance, the SG downlink capacity is a fixed bottleneck in the original system which equals the sum of RAO data rate and SCS throughput. On the other hand, the allocation of additional resources changes the bottleneck of the throughput. In FDD mode, when the number of satellites decreases from 5 to 2, the bottleneck link of SCS changes from the SG link to the US link for RAO data rate less than 1.9 Gbps. In TDD mode, the slopes of the curves decrease when the RAO data rate is less than 4.3 Gbps (3.6 Gbps) for the case of $M = 2$ ($M = 5$) because of the optimal allocation of new resources between the four links.

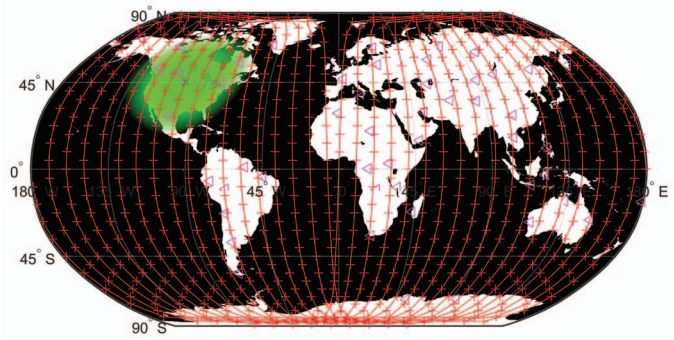

Fig. 4. An example of an RAO area (green disk projected on the earth surface) for data transport design where snap-short locations of LEO satellites are denoted by $+$ and earth-station gateways are denoted by $\triangle$.

IV. RAO Data Transport Design

A. Development of Data Transport

An RAO mission in the proposed paradigm involves both the observation and the data transport. To specify an RAO mission, we define three parameters: i) the center of observation area $\mathcal{C}$ on the NGSO surface, ii) the observation radius R_{ob} and iii) the selected gateway number L. $\mathcal{C}$ and R_{ob} specify a circle region within which the radio telescopes conduct the RAO mission. The L nearest gateways to the observation center $\mathcal{C}$ are selected for RAO data downlink transmission. In other words, the parameters $\mathcal{C}$, R_{ob} and L define the RAO data sources and the destinations so that the RAO data transferring problem can be analyzed.

Since both the satellites and the Earth rotate, our analysis is based on a single snapshot or short-time model. To be more specific, we show the projected locations of the LEO satellites, the gateways and the RAO region on the world map in Fig. 4. Particularly, the lands are represented in white and the ocean areas are in black, the gateways, the satellites and the orbits are shown as symbols '$\triangleleft$', '+' and red curves respectively. The projected RAO area is shown as the green disk in Fig. 4.

For the RAO data transport design, we consider the SG transmissions which involve L selected gateways and N_d gateway-connected satellites. The connections between satellites and gateways are based on the nearest neighbor criterion. The number of satellites an earth-station gateway can simultaneously connect generally depends on the number of antennas co-located at the gateway as well as the satellite constellations and gateway location. For the OneWeb system, a gateway can have 10 antennas (or more in some cases) while there are more then 10 satellites in the gateway's view [21]. Thus, in our evaluation, we assume a gateway connects to at most the nearest 10 satellites above the minimum elevation angle and the satellite selects the nearest gateway to set up a two-way connection. Based on this model, we will study how the RAO data rate interacts with the SCS traffic and then solve the RAO data transport problem. We note that although this model is only based on a snapshot, our analysis can also be extended to consider the problem during certain time periods in that the selection of gateways can be managed to guarantee fixed SG connections for a certain period.

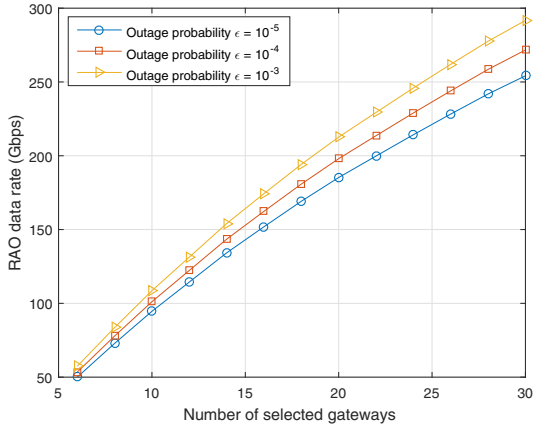

Fig. 5. RAO data rate versus the number of selected gateways

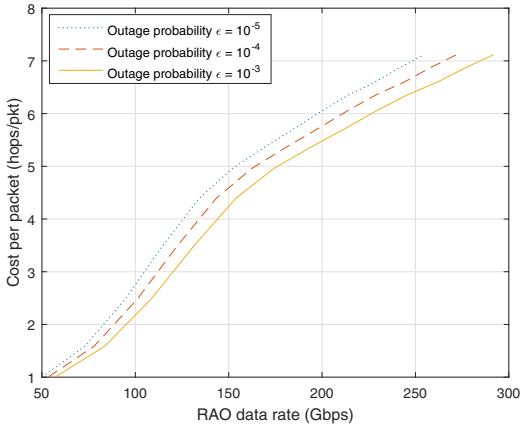

Fig. 6. RAO data packet relaying cost

We assume the downlink traffic of the ith satellite is represented as a Poisson random variable x_i (packets per second) [24]–[27] with a mean value of λ_i, where $i = 1, \ldots, N_d$. We now propose a simple strategy for the RAO data downloading while guaranteeing the SC data transmission through the SG links within a required outage probability constraint. Specifically, to guarantee an outage probability constraint of ϵ for the ith satellite connected to the selected gateway, a traffic level of $\bar{K}_i = F_K^{-1}(1-\epsilon, \lambda_i)$ should be supported, corresponding to a data rate of $\gamma_{\rm SG}\bar{K}_i$. In addition, the capacity of the total SG links can be dynamically changed according to the number of satellites connected to the gateway. In other words, the gateways are equipped with multiple antennas and can perfectly reuse the spectrum for different SG links. Therefore, given the capacity of the ith SG link $\tilde{C}_{{\rm SG},i}$, the following residual data rate can be used for RAO data downloading:

$$R_{{\rm RAS},i} = \max\left\{\tilde{C}_{{\rm SG},i} - \gamma_{\rm SG}\bar{K}_i,\ 0\right\}, \quad i = 1, \ldots, N_d. \tag{15}$$

Thus, the total supportable RAO data rate is $R_{\rm RAS} = \sum_{i=1}^{N_d} R_{{\rm RAS},i}$. Note that a larger $R_{\rm RAS}$ can also be supported by using more gateways or at the cost of either higher SCS outage probability or smaller SCS average throughput using the same number of gateways.

Considering that satellites within the RAO region may have different RAO data rates and that the selected gateways may also have different traffic levels, we now discuss the problem of allocating the RAO data rate to the selected gateways to minimize the total RAO data relaying cost. To be specific, we assume there are N_s satellites located within the RAO region with data rates $\{s_j,\ j = 1, \ldots, N_s\}$. We guarantee $\sum_{j=1}^{N_s} s_j = R_{\rm RAS}$ so that the source and destination RAO data rates are balanced.

We select L gateways for RAO data downloading and then the N_d satellites connected to the selected gateways can be specified according to the nearest neighbor criterion. We say these N_d satellites are the destinations for the N_s sources (satellites) generating RAO data. A simple example of the connectivities among the involved satellites and gateways is shown in Fig. 2(b) to illustrate the considered problem. Different source and destination pairs may need different numbers of ISL hops. Denoting the data flow (packets per second) from the jth source to the ith destination as $f_{j,i}$, our goal is to minimize the total cost of relaying the RAO data by optimally allocating the flows between the sources and the destinations. To simplify the problem, we assume there is no maximum rate constraint to the RAO data flow in ISLs. Therefore, the minimum cost RAO data flow allocation problem can be formulated as

$$\min_{\{f_{j,i}\}} \quad \sum_{j=1}^{N_s}\sum_{i=1}^{N_d} c_{j,i} f_{j,i} \tag{16a}$$

$$\text{s.t.} \quad \sum_{j=1}^{N_s} f_{j,i} = R_{{\rm RAS},i}, \quad i = 1, \ldots, N_d \tag{16b}$$

$$\sum_{i=1}^{N_d} f_{j,i} = s_j, \quad j = 1, \ldots, N_s \tag{16c}$$

$$0 \le f_{j,i}. \tag{16d}$$

where $c_{j,i}$ is the cost to relay an RAO data packet from the jth source satellite to the ith destination satellite. The cost between a source and a destination is counted as the minimal number of hops (satellites) the flow passes through. We can recognize this flow allocation problem is a linear programming problem which can be solved with some existing softwares such as MATLAB.

B. Data Transport Performance Results

In the simulation, we assume the RAO region is centered at 45°N 100°W with an observation radius $R_{\rm ob} = 3000$ km which is shown as the green area in Fig. 4. We apply the same FDD settings mentioned in Section III for all the L selected gateways. In addition, for the N_d satellites connected to the selected gateway, we generate their mean traffic values from a Poisson distribution. The simulation results are based on the average of 100 realizations of the random locations of the gateways (where the minimum distance between any two gateways are 1029 km) and of 100 realizations of the Poisson distributed traffics (where the means are generated from a Poisson distribution with the mean of 1500 packets/s). For

simplicity, we also assume all the sources generate the same RAS data rate, i.e., $s_j = R_{\mathrm{RAS}}/N_s,\ j = 1, \ldots, N_s$. Then, we analyze the relationship among the number of selected gateways, the supportable RAO data rates and the cost of RAO data transport under different outage probability requirements to the SCS.

The simulation results are shown in Fig. 5 and Fig. 6. Specifically, Fig. 5 indicates that i) for the same outage probability constraint, the total RAO data rate grows as the number of selected gateways increases and ii) for the same number of selected gateways, guaranteeing smaller SCS outage probability results in lower RAO data rate. Similarly, in Fig. 6 we can see that the cost of relaying a packet from the source to the destination grows with the increase of the RAO data rate. On the other hand, the slope of the curves varies as the RAO data rate increases. The reason is that as the RAO data rate increases, more gateways at farther locations from the sources are needed to accommodate the RAO data downloading. Although the gateways are uniformly distributed on lands, the lands themselves are not uniformly distributed, i.e., isolated by oceans, which results in a non-constant slope of the curves. Furthermore, Fig. 6 indicates that for the same RAO data rate, smaller SCS outage probability requirement results in higher cost.

V. Conclusions

In this paper, we proposed a new paradigm for NGSO satellite communication system (SCS) and radio astronomy system (RAS) which benefits both systems significantly. This innovation provides the NGSO SCS with not only additional frequency resources but also new business opportunities. Besides, the RAS can obtain plenty of opportunities for the RAS observations in new bands and avoid RFI from the devices below the orbit. We discussed potential deployment scenarios, advantages and challenges of the proposed paradigm. We developed a resource allocation design for the integrated NGSO SCS and RAS system which maximizes the SCS throughput while providing a guaranteed RAO data rate support. Furthermore, we presented a RAO data transport design which minimizes the inter-satellite relaying cost. Our results show that a new additional spectrum with TDD offers more flexible resource allocation in overcoming the link bottleneck. The number of gateways used for RAO data downloading can be adjusted to provide desired RAO data rate and SCS throughput. Overall, the proposed NGSO-based integrated SCS and RAS system opens up a promising new era for SCS and RAS.

Acknowledgment

This material is based upon work supported by the National Science Foundation under Grant No. 1547048.

References

[1] J. Lim, R. Klein, and J. Thatcher, "Good technology, bad management: A case study of the satellite phone industry," *J. Inform. Technol. Management*, vol. 16, no. 2, pp. 48–55, 2005.

[2] O. Nizhnik, "A low-cost launch assistance system for orbital launch vehicles," *Intl. J. Aerospace Engineering*, vol. 2012, 2012.

[3] J. Straub, "Cubesats: A low-cost, very high-return space technology," in *Proc. 2012 Reinventing Space Conf.*, 2012.

[4] W. Hanson, "A global Internet: The next four billion users," *New Space*, vol. 3, no. 3, pp. 204–207, 2015.

[5] V. L. Foreman, A. Siddiqi, and O. De Weck, "Large satellite constellation orbital debris impacts: Case studies of OneWeb and SpaceX proposals," in *AIAA SPACE and Astronautics Forum and Exposition*, 2017, p. 5200.

[6] U. Siddique, H. Tabassum, E. Hossain, and D. I. Kim, "Wireless backhauling of 5G small cells: challenges and solution approaches," *IEEE Wireless Communications*, vol. 22, no. 5, pp. 22–31, 2015.

[7] S. W. Ellingson, J. D. Bunton, and J. F. Bell, "Removal of the GLONASS C/A signal from OH spectral line observations using a parametric modeling technique," *The Astrophysical Journal Supplement Series*, vol. 135, no. 1, p. 87, 2001.

[8] B. D. Jeffs, L. Li, and K. F. Warnick, "Auxiliary antenna-assisted interference mitigation for radio astronomy arrays," *IEEE Trans. Signal Process.*, vol. 53, no. 2, pp. 439–451, 2005.

[9] ITU-R, "Techniques for mitigation of radio frequency interference in radio astronomy," Sept. 2013.

[10] A. M. Sardarabadi, A.-J. Van Der Veen, and A.-J. Boonstra, "Spatial filtering of RF interference in radio astronomy using a reference antenna array," *IEEE Trans. Signal Process.*, vol. 64, no. 2, pp. 432–447, 2016.

[11] H. Minn, Y. R. Ramadan, and Y. Dai, "A new shared spectrum access paradigm between cellular wireless communications and radio astronomy," *Proc. GLOBECOM, IEEE*, 2016.

[12] Y. R. Ramadan, H. Minn, and Y. Dai, "A new paradigm for spectrum sharing between cellular wireless communications and radio astronomy systems," *IEEE Trans. Commun.*, vol. 65, no. 9, pp. 3985–3999, Sept. 2017.

[13] M. E. Abdelgelil and H. Minn, "Non-linear interference cancellation for radio astronomy receivers with strong RFI," *Proc. GLOBECOM, IEEE*, 2017.

[14] Tallinn, "Impact of unwanted emissions of Iridium satellites on radioastronomy operations in the band 1610.6-1613.8 MHz, ECC REPORT 171," Oct. 2011.

[15] T. L. Wilson, K. Rohlfs, and S. Hüttemeister, *Tools of radio astronomy*. Springer, 2009, vol. 5.

[16] H. Hirabayashi *et al.*, "The VLBI space observatory programme and the radio-astronomical satellite HALCA," *Publications of the Astronomical Society of Japan*, vol. 52, no. 6, pp. 955–965, 2000.

[17] N. Kardashev *et al.*, "RadioAstron-A telescope with a size of 300 000 km: Main parameters and first observational results," *Astronomy Reports*, vol. 57, no. 3, pp. 153–194, 2013.

[18] D. Han and H. Minn, "Performance analysis of distributed radio telescopes under shared spectrum access paradigm," *Proc. GLOBECOM, IEEE*, 2017.

[19] ——, "Performance analysis of distributed auxiliary radio telescopes under shared spectrum access paradigm and cooling power constraint," *IEEE Access*, vol. 5, pp. 21 709–21 722, 2017.

[20] VAO LLC. US Virtual Astronomy Observatory. [Online]. Available: http://www.usvao.org/index.html

[21] OneWeb. (2013) OneWeb Non-Geostationary Satellite System Attachment A. [Online]. Available: https://licensing.fcc.gov/myibfs/download.do?attachment_key=1134939

[22] FCC. (2017, August) FCC online table of frequency allocations. [Online]. Available: https://transition.fcc.gov/oet/spectrum/table/fcctable.pdf

[23] ——, "Order and Declaratory Ruling, FCC 17-77," June 2017.

[24] G. McMahon, R. Septiawan, and S. Sugden, "A multiservice traffic allocation model for LEO satellite communication networks," *IEEE J. Selected Areas Commun.*, vol. 22, no. 3, pp. 501–507, 2004.

[25] C. Chen and E. Ekici, "A routing protocol for hierarchical LEO/MEO satellite IP networks," *Wireless Networks*, vol. 11, pp. 507–521, 2005.

[26] W. Jiang and P. Zong, "A discrete-time traffic and topology adaptive routing algorithm for LEO satellite networks," *Intl J. Commun., Network and System Sciences*, vol. 4, pp. 42–52, 2011.

[27] W. Lin, Z. Deng, Q. Fang, N. Li, and K. Han, "A new satellite communication bandwidth allocation combined services model and network performance optimization," *Intl. J. Satellite Commun. and Networking*, vol. 35, no. 3, pp. 263–277, 2017.